JOURNAL OF AGRICULTURAL AND FOOD CHEMISTRY

Myowater Dynamics and Protein Secondary Structural Changes As Affected by Heating Rate in Three Pork Qualities: A Combined FT-IR Microspectroscopic and ^{1}H NMR Relaxometry Study

ZHIYUN WU,*,† HANNE CHRISTINE BERTRAM,† ULRIKE BÖCKER,‡ RAGNI OFSTAD,‡ AND ACHIM KOHLER‡,§

Department of Food Science, Faculty of Agricultural Sciences, University of Aarhus, Research Centre Foulum, P.O. Box 50, DK-8830 Tjele, Denmark, Center for Biospectroscopy and Data Modelling, Matforsk AS, Norwegian Food Research Institute, Osloveien 1, NO-1430 Ås, Norway, and CIGENE—Center for Integrative Genetics and Department of Mathematical Sciences and Technology (IMT), University of Life Sciences, 1432 Ås, Norway

The objective of this study was to investigate the influence of heating rate on myowater dynamics and protein secondary structures in three pork qualities by proton NMR T_2 relaxation and Fourier transform infrared (FT-IR) microspectroscopy measurements. Two oven temperatures at 100 °C and 200 °C corresponding to slow and fast heating rates were applied on three pork qualities (DFD, PSE, and normal) to an internal center temperature of 65 °C. The fast heating induced a higher cooking loss, particularly for PSE meat. The water proton T_{21} distribution representing water entrapped within the myofibrillar network was influenced by heating rate and meat quality. Fast heating broadened the T_{21} distribution and decreased the relaxation times of the T_{21} peak position for three meat qualities. The changes in T_{21} relaxation times in meat can be interpreted in terms of chemical and diffusive exchange. FT-IR showed that fast heating caused a higher gain of random structures and aggregated β-sheets at the expense of native α-helixes, and these changes dominate the fast-heating-induced broadening of T_{21} distribution and reduction in T_{21} times. Furthermore, of the three meat qualities, PSE meat had the broadest T_{21} distribution and the lowest T_{21} times for both heating rates, reflecting that the protein aggregation of PSE caused by heating is more extensive than those of DFD and normal, which is consistent with the IR data. The present study demonstrated that the changes in T_2 relaxation times of water protons affected by heating rate and raw meat quality are well related to the protein secondary structural changes as probed by FT-IR microspectroscopy.

KEYWORDS: FT-IR spectroscopy; NMR; T_2 relaxation; protein secondary structure; cooking rate; water dynamics; meat

INTRODUCTION

The effect of cooking procedure on final meat quality is mainly determined by the distribution of myowater and the structure of meat proteins, the two main constituents of meat. Both constituents have a synergistic effect on meat quality since the majority of water is located in the myofibrillar framework, and changes in the protein structure in meat are supposed to be significantly associated with the changes in water distribution. The meat proteins undergo substantial structural changes and suffer water loss upon heating, and this affects the quality of meat product (*1*).

Heating temperature, heating rate, and raw meat quality are highly related to the final meat quality in terms of cooking loss, juiciness, and tenderness. Effects of heating rate on cooking loss and sensory properties have been extensively investigated. A slow heating rate resulted in a significantly lower cooking loss, increased yield, and improved juiciness and tenderness (*2*−*5*) compared with a high heating rate. No effect of heating rate on cooking loss was found for lean ground beef (*6*). It was also demonstrated that fast heating compared with slow heating caused more severe myofibrillar shortening (*7*) and decreased sarcomere length (*8*). Furthermore, a lower cooking loss upon heating rate was observed in meat with a high ultimate pH when compared with a low ultimate pH (*5*). However, the effect of heating rate on the functional quality of meat has only been scarcely studied on the molecular level using

* To whom correspondence should be addressed. Phone: (45) 89 99 1142. Fax: (45) 89 99 1564. E-mail: Zhiyun.Wu@agrsci.dk.
† University of Aarhus.
‡ Norwegian Food Research Institute.
§ University of Life Sciences.

10.1021/jf070019m CCC: $37.00
Published on Web 04/24/2007

Fourier transform infrared (FT-IR) microspectroscopy and water proton NMR T_2 relaxation times.

FT-IR spectroscopy probes molecular structure on the basis of IR energy absorption of chemical bonds at the specific frequencies related to molecular vibration. FT-IR can provide both qualitative and quantitative analysis of functional groups. FT-IR microspectroscopy has been applied in meat science to study denaturation processes in myofibrillar and connective tissue proteins in beef (*9*) and the changes in myofibrillar protein structure of pork as affected by heating, salting, and aging (*10*−*12*). An increase in aggregated β-sheet and a decrease in α-helical structures on heating have been observed much more pronounced for the myofibers than for the connective tissue using FT-IR imaging (*9*). Salting induced an increase in native β-sheet and a decrease in α-helical structures while aging triggered an increase in native α-helical structure before heating (*12*). The use of water proton NMR T_2 relaxation times in meat has been successful because of its potential in charactering water and structural features (*13*). Perturbations in the T_2 relaxation times do not only reflect the structural changes of muscle but also the changes in water mobility, the interaction between water and macromolecules, and the water distribution in meat. It has been found that an increase in ^{1}H NMR T_2 relaxation times and the promoted water uptake caused by the interaction of aging time and salting are related to an increase in native β-sheet structure induced by salting and an increase of native α-helical structure induced by aging, whereas a decrease in T_2 relaxation times and broadening of T_2 distribution upon heating are attributed to the increase of aggregated β-sheet structure (*10*, *12*).

The objective of this study was to elucidate the influence of heating rate on the water proton transverse relaxation time T_2 and on meat myofiber protein secondary structural changes in three pork qualities using a combined low-field NMR relaxometry and FT-IR microspectroscopy study. It is aimed to construct a relationship between water distribution and meat protein structural changes upon heating rate for different meat qualities.

MATERIALS AND METHODS

Animals and Sampling. Three pigs, which were offspring of Duroc/Landrace boars crossbred with Landrace/Yorkshire sows, were used in this study to obtain three different meat qualities (DFD, PSE, and normal). DFD meat was obtained from a pig injected with adrenaline (subcutaneous injection, 0.2 mg/kg live weight) 16 h before slaughter to increase the final pH of the meat as described previously (*14*). PSE meat was obtained from a pig that was exercised on a treadmill at a speed of 3.8 km/h for 22 min immediately prior to electrical stunning. The normal meat was obtained from a pig without any special treatment. The three pigs were slaughtered on 3 days in the experimental abattoir at Research Centre Foulum. The adrenaline-treated and the control pigs were stunned by 80% CO_2 for 3 min, while the treadmill-exercised pig was electrically stunned. Following stunning, all pigs were exsanguinated and scalded at 62 °C for 3 min. Cleaning and evisceration of the carcass were completed within 30 min postmortem. The carcass was split and kept at 12 °C. Within 3 h postmortem, the carcass was transferred to a chill room, where it was stored at 4 °C.

At both 45 min and 24 h postmortem, pH was measured in the left M. longissimus muscles of the three meat qualities (**Table 1**). Drip loss of the M. longissimus muscles of each pig was measured after 24 h postmortem using Honikel's bag method (*15*) (**Table 1**). The samples for drip loss were taken from the posterior end of the muscles. The measured pH and drip loss demonstrated very well that meat used in this study is representative for each meat quality. Both the right and the left M. longissimus of each pig were excised 24 h postmortem and were cut into eight parallel chops of ca. 10 cm, and each chop was weighed out (W1) before heating.

Table 1. Meat pH Values Measured 45 min and 24 h Postmortem and Drip Loss of Three Raw Meat Qualities

raw meat quality	pH (45 min postmortem)	pH (24 h postmortem)	drip loss (%)
DFD	6.7	6.2	2.0
PSE	6.3	5.7	7.4
normal	6.7	5.7	4.1

Heating. The two heating rates were controlled by adjusting the oven temperature to 100 °C and 200 °C. Four chops from each pig (two from the right and two from the left M. longissimus muscles) were used for one heating rate, while the remaining four chops were used for the other heating rate. Thermal meters (PT 100, Labfacility, United Kingdom) were inserted into the geometric center of meat samples. When the internal center temperature of meat reached a temperature of 65 °C, the roasts were removed from the oven. After the meat roasts were cooled to ambient temperature, the roasts were weighed out again (W2) and cooking loss was calculated according to the following equation (eq 1):

$$\text{cooking loss (\%)} = \frac{\text{weight1} - \text{weight2}}{\text{weight1}} \times 100 \qquad (1)$$

^{1}H NMR T_2 Relaxation Time Measurements. Five NMR samples with a size of approximately 1 × 1 × 4 cm were cut from the approximately geometric center area of each roast. Accordingly, 20 samples were obtained for each combination of meat quality and heating rate, resulting in a total of 120 samples for NMR measurements. The ^{1}H NMR T_2 relaxation time measurements of all 120 samples were performed at 25 °C on a Maran Benchtop Pulsed NMR Analyzer (Resonance Instruments, Witney, U.K.) with a resonance frequency for protons of 23.2 MHz. The NMR instrument was equipped with an 18 mm variable temperature probe. Transverse relaxation (T_2) was measured using the Carr−Purcell−Meiboom−Gill sequence (CPMG). The T_2 measurements were performed with a τ-value (time between 90° pulse and 180° pulse) of 150 μs and using a repetition delay of 3 s. Data were acquired as the amplitude of every second echo (to avoid influence of imperfect pulse settings) in a train of 4096 echoes as an average of 16 repetitions. After NMR relaxation measurements, the samples were divided into subsamples, were snap-frozen in liquid N_2, and were preserved at a temperature of −80 °C for FT-IR spectroscopy measurements.

The obtained NMR transverse relaxation decays were analyzed by distributed exponential fitting analysis, which was performed according to the regularization algorithm of Butler, Reeds, and Dawson (1981) and were implemented in the RI Win-DXP software program (release version 1.2.3) from Resonance Instruments Ltd, United Kingdom. This analysis yields a plot of relaxation amplitude for individual relaxation processes versus relaxation time. Using an in-house program written in Matlab (The Mathworks Inc., Natick, MA), peak positions of the found relaxation populations were determined, and corresponding areas were calculated by integration.

FT-IR Measurements. FT-IR measurements were performed with an IR microscope II (Bruker Optics, Germany), coupled to an Equinox 55 spectrometer (Bruker Optics, Germany). The microscope was equipped with a computer-controlled *x*,*y* stage. The Bruker system was controlled with an IBM compatible PC running OPUS-NT software. Tissue cryosections of 10 μm thickness were thaw-mounted on CaF_2 substrates. The samples were dried in a desiccator using anhydrous silica gel to minimize the contribution of water absorption in IR. Purging of the sample compartment with dry air was applied to reduce water vapor. The spectra were recorded from single fibers in the region between 4000 and 600 cm^{-1} with a spectral resolution of 6 cm^{-1} using a mercury−cadmium−tellurium detector and an aperture of 5.0 mm. For each spectrum, 256 scans were accumulated and averaged. Eight NMR subsamples for each heating rate on one meat quality were used for FT-IR spectra measurements. From each subsample, three spectra were collected, resulting in a total of 144 spectra for all six experimental conditions. The original IR spectra between 4000 and 600 cm^{-1} were preprocessed by extended multiplicative signal correction (EMSC) using

Table 2. Cooking Loss, T_{21} Width, and T_{21} Peak Position for the Different Combinations of Meat Quality and Heating Rate

	normal slow	normal fast	DFD slow	DFD fast	PSE slow	PSE fast	standard error	*P*-value meat quality	*P*-value heating rate
cooking loss (%)	14.2	25.1	12.7	26.3	21.1	29.3	0.8	0.0003	<0.0001
T_{21} width (ms)	17.8	20.1	19.1	20.2	22.3	23.5	0.6	<0.0001	0.0032
T_{21} peak position (ms)	34.1	33.1	30.9	28.9	28.6	27.6	0.5	<0.0001	0.0044

The Unscrambler (Camo Process AS, Oslo, Norway) version 9.2 to avoid the physical light-scattering effects (*16*, *17*). After EMSC, the second derivative of the spectra was taken to resolve overlapping of bands. After preprocessing, the spectra from the same experimental condition were averaged.

Data Analysis. To analyze the main variation in the datasets and the correlation between the design parameters (heating rate and raw meat quality) and the FT-IR absorbance bands, the data analysis was performed using principal component analysis (PCA) and analysis of variance (ANOVA) by partial least-squares regression (PLSR2) of The Unscrambler version 9.2. PLSR2 is a two-block, bilinear data approximation method, where a matrix of response variables **Y** is predicted by a matrix **X**. It is based on so-called latent variables, that is, the methods aim at finding new directions in the variable space of **X** using only the most relevant part of the matrix **X** for the prediction of **Y** (*18*). The new directions are called PLS components and are linear combinations of all **X**-variables. In ANOVA PLSR, the design variables are defined as indicator variables weighted by their standard deviations and are used as **X**-matrix. The relationship between the design variables and the FT-IR variables can be studied by correlation loading plots (*18*).

The relationship between protein secondary structures assessed by FT-IR microspectroscopy and NMR T_2 relaxation times was elucidated by the correlation loading plots of PLSR2 using the design parameters (heating rate and meat quality) and T_2 relaxation times as **X**-matrix and FT-IR bands as **Y**-matrix (*19*). The design variables were used as indicator variables and were down-weighted so that they do not influence the PLSR model.

Traditional statistical analyses of the data were carried out with the SAS software version 8.2 (SAS Institute Inc., Cary, NC). The statistical model used was the PROC GLM procedure. The statistical models for the cooking loss, the width of water proton T_{21} distribution, and the peak position of water proton T_{21} distribution included the fixed effects of heating rate and raw meat quality.

RESULTS AND DISCUSSION

Cooking Loss. The cooking loss for the two heating rates and three raw meat qualities is presented in **Table 2**. The heating rate showed significant effects on cooking loss. Fast heating induced a significantly higher cooking loss than slow heating regardless of the raw meat quality, which is consistent with previous studies (*2*−*5*). A severe myofibrillar shortening (*7*) and decreased sarcomere length (*8*) caused by fast heating may be the explanation for the higher cooking loss. Of the three meat qualities, PSE meat had a higher cooking loss than normal and DFD meat for both heating rates. Similar observations have been found earlier that PSE meat lost significantly more liquid than normal or DFD meats during cooking of pork (*20*), and a lower cooking loss upon heating rate was observed in meat with a high ultimate pH compared with a low ultimate pH (*5*). It is well-known that because of a high rate of postmortem glycolysis, PSE meat experiences a low pH when temperature is still high. Subsequently, PSE meat was characterized by a higher amount of drip loss, a higher level of protein denaturation (*21*−*24*), and larger intercellular spaces among muscle fibers and bundles (*25*) compared with DFD and normal meat. All these structural differences of PSE meat may lead to the higher cooking loss found in PSE meat. However, the variation of cooking loss caused by heating rate has been scarcely studied with relation to NMR T_2 relaxation times and protein secondary structure.

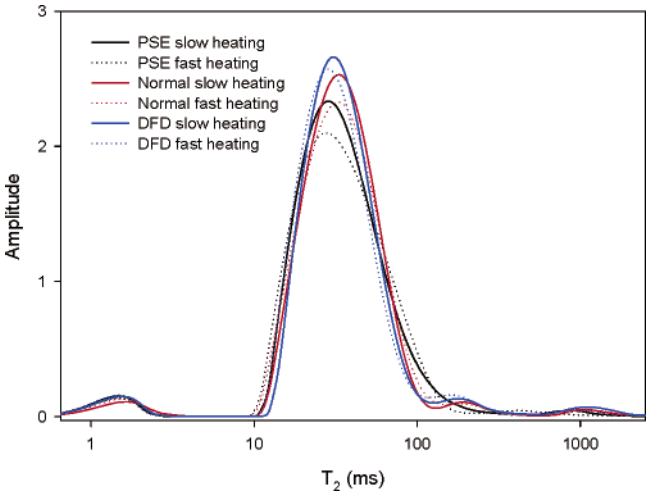

Figure 1. Distributed water proton NMR T_2 relaxation times of three meat qualities heated by two heating rates. Each curve represents the average of 20 measurements.

In the present study, the effects of heating rate and meat quality on cooking loss were demonstrated to be in high correlation with the changes in water proton T_2 relaxation times in meat. This is well explained by the changes in protein secondary structures, which is discussed in the following parts.

Water Proton NMR T_2 Relaxation Times. The distributed water proton NMR T_2 relaxation times of three raw meat qualities heated by two heating rates are shown in **Figure 1**. Each curve represents the average of 20 samples from both left and right M. longissimus muscles. The major T_2 population was located in the region of 10−140 ms (T_{21}) representing the major water population that is entrapped within the myofibrillar network, and two minor T_2 populations centered at 1−2 ms (T_{2B}) and 1000 ms probably represent the water tightly associated with macromolecules and the exuded water near or at the surface of the meat, respectively (*13*). Statistical analysis revealed that changes in T_{21} distribution depended on both heating rate and meat quality. Since it is well-known that T_{21} reflects the majority of water in meat, emphasis is put on the analysis and explanation of changes in T_{21} caused by heating rate and raw meat quality. **Table 2** shows the width and peak position of the T_{21} distribution of three raw meat quality samples heated by two heating rates. Statistical analyses revealed that heating rate had a significant effect on both the width and position of the T_{21} population. Fast heated meat samples showed a broader distribution of T_{21} relaxation times and lower relaxation times of T_{21} peak position than slowly heated samples for each of three meat qualities. Furthermore, of the three meat qualities, PSE meat had the broadest T_{21} distribution and the lowest T_{21} relaxation times for both heating rates. However, no significant difference in the width of the T_{21} distribution was observed between normal and DFD meat when fast heated. In addition, only a minor difference in the peak position of T_{21} distribution was found between fast heated DFD and slow heated PSE meat.

The variation in water proton T_{21} relaxation times can be ascribed to meat protein structural changes caused by heating

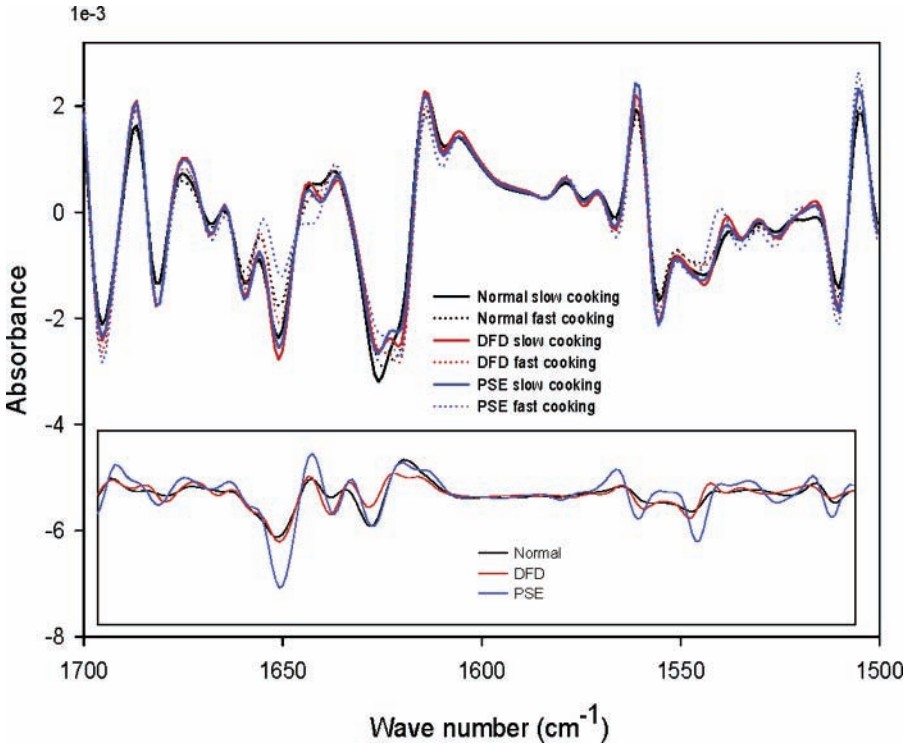

Figure 2. Second derivative of the FT-IR spectra for the different combinations of heating rate and meat quality in the region of 1700–1500 cm^{-1}. Prior to taking the second derivative, the spectra were preprocessed by EMSC. Each curve represents the average of 24 measurements. The insertion denotes the spectral differences between slow and fast heating rates for three meat qualities.

rate. A relationship between the relaxation time of T_{21} and sarcomere length/myofilament lattice has been observed, and it was suggested that the ratio between the I- and A-band determines the relaxation time of T_{21} (*26*). It has also been demonstrated that heating generally deceases the T_2 times and broadens the T_2 distribution of normal quality meat because of the thermal denaturation (*10*, *12*), and T_2 relaxation times differed significantly between PSE, DFD, and normal meat (*5*, *27*). In this study, the changes in T_2 upon heating rate are expected to reflect the different extent of meat structural changes because of the different heating rate. The broader T_{21} distribution and lower relaxation time of the T_{21} peak position upon fast heating compared with slow heating indicate that fast heating produces larger spatial variation in protein structure and a more severe protein aggregation because of the thermal denaturation. Furthermore, the broadest T_{21} distribution and the lowest relaxation time of the T_{21} peak position for fast heated PSE meat indicate that PSE meat had undergone more significant protein aggregation than normal and DFD meat during fast heating. This may be related to the structural features of PSE meat. However, the similarity in the width of T_{21} distribution between fast heated normal and DFD meat may suggest that normal and DFD meat experience the similar extent of meat protein aggregation upon fast heating.

The changes in the distribution of T_2 relaxation times and their relationship with meat protein structure may explain cooking loss and sensory property upon heating rate and meat quality. The high cooking loss induced by fast heating is ascribed to the more significant protein aggregation that takes place during fast heating, which corresponds to the broad T_{21} distribution and low T_{21} value at the peak position caused by fast heating. Moreover, PSE meat had a higher cooking loss for both heating rates, which accords with the broader T_{21} distribution and lower relaxation time of the T_{21} peak position of PSE meat than those of DFD and normal meat. The sensory properties such as juiciness and tenderness upon heating rate have previously been studied (*2*, *3*, *5*, *7*). Enhanced juiciness and tenderness were found for meat cooked by a slow heating rate. However, the enhanced sensory properties at a slow heating rate have only been scarcely explained with relation to the water proton T_2 relaxation times. The present study indicates that a narrow T_{21} distribution and a high relaxation time of the T_{21} peak position reflecting less aggregation of protein and more water content may be related to a high juiciness and tenderness of slowly heated meat. Consequently, links between the variation of T_{21} relaxation times and cooking loss, sensory property, and meat protein structural changes upon heating rate can be proposed. A relatively narrow T_{21} distribution and a high relaxation time of the T_{21} peak position indicate a relatively high water content, less protein denaturation, and improved sensory property of slowly heated meat at least up to 65 °C. This relationship is in agreement with an earlier study where a high final cooking temperature was found to affect the distributed T_2 relaxation times in a way identical to fast heating in the present study, and where this was found to result in reduced juiciness (*28*). Accordingly, the distribution of water proton T_2 relaxation times is a good indicator of meat protein structure and meat functional properties after meat processing.

Water proton transverse relaxation times are not only related to the meat protein structure but also to the water dynamics and the interaction between water and macromolecules in the meat structure. The changes in water proton transverse relaxation behavior in bovine serum albumin and biopolymer solution and gels can be interpreted in terms of chemical and diffusive exchange (*29*−*32*). Aggregation reduces the protein proton T_2 relaxation times because the dipolar−dipolar interaction between protein protons is no longer averaged by rotational motion. The decreased water proton T_2 relaxation times can be explained by the chemical exchange of water protons with protein protons. Water proton relaxation in milk protein mixtures was also found

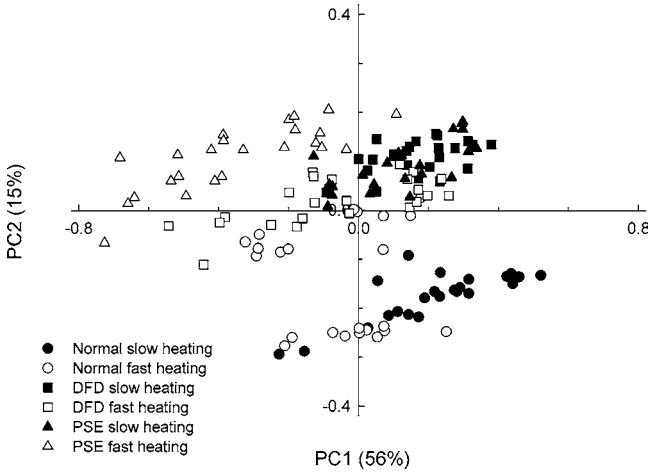

Figure 3. PCA score plots of 144 samples using the IR spectra in the region of 1700–1500 cm^{-1} as variables. The explained variance by PC1 and PC2 is 56% and 15%, respectively.

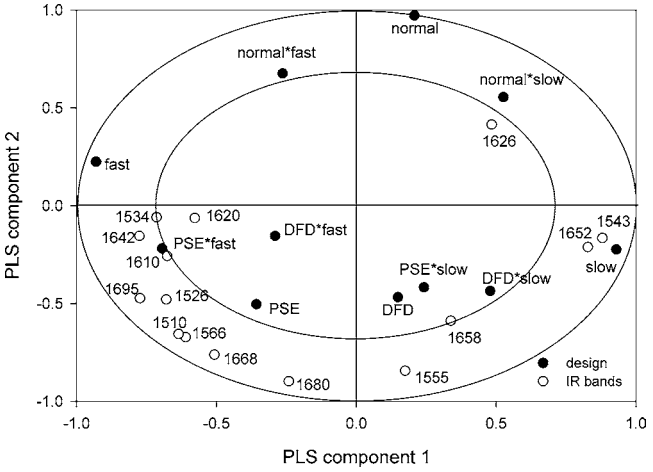

Figure 4. Correlation loading plot (first and second PLS component) of PLSR2 using design parameters (heating rate, meat quality, and interaction) as *X* and selected frequency variables of the (negative) second derivative of FT-IR spectra in the region of 1700–1500 cm^{-1} as *Y*. The inner and outer ellipses refer to 50% and 100% explained variance in *X* and *Y*, respectively. The validated explained variances are 32%/25% for *X* and 47%/17% for *Y*, the first and the second component, respectively.

to integrate the participation of exchangeable protons of macromolecules in water relaxation (*33*). ^1H NMR T_2 relaxation in meat is also proposed to be sensitive to the chemical exchange mechanism because water accounts for approximately 70−75% of meat weight. We propose that chemical exchange between water protons and protein protons in meat contributes to the faster relaxation rate of myowater in fast heated compared with slowly heated meat. Fast heating induced a much more severe meat protein aggregation and in turn longer correlation times of most protein protons, and myowater protons experienced faster relaxation rates because of the chemical exchange between protein protons and water protons. Furthermore, protein protons associated with different protein conformation show different correlation times and hence different exchange rates with water protons. As a result of the complexity of meat protein conformation and severe protein structural changes after heating, particularly after fast heating, the broadening of the T_{21} distribution is subsequently significant after fast heating up to an internal temperature of 65 °C. On the other hand, it demonstrated that the width of T_{21} distribution reflects the extent of heterogeneity of meat protein structure, which was further confirmed by a decrease in the width of T_{21} distribution at much higher temperatures, at which myosin and sarcoplasmic proteins may be completely denatured.

FT-IR Microspectroscopy. Figure 2 shows the second derivative of the FT-IR spectra for the different combinations of heating rate and raw meat quality in the amide I and amide II region of 1700−1500 cm^{-1}. Prior to taking the second derivative, the spectra were preprocessed by EMSC. Each curve represents the average of 24 measurements and the minima in the second derivatives correspond to the maxima in the original spectra. Significant changes in the intensity of a strong absorption band at 1652 cm^{-1} were observed, which is well-known to arise from α-helical structures in amide I region. Slowly heated samples had more α-helical structures than fast heated samples, and PSE meat samples exposed to fast heating rate had the least α-helical structures. The band at 1543 cm^{-1} was also observed to be positively related to the slow heating, which is assigned to the α-helical structures in the amide II region (*34*−*35*). The strong bands at 1626 and 1620 cm^{-1} may both arise from the aggregated intermolecular *β*-sheets. However, the band at 1626 cm^{-1} showed a high intensity for slowly heated meat and the band at 1620 cm^{-1} had a high intensity for fast heated meat. The insertion in **Figure 2** presents the spectral differences between slow and fast heating rates for three meat qualities, which indicate the different extent of effect of heating rate on protein secondary structures for different raw meat qualities. To observe the main variations in IR spectra of 144 samples within the region of 1700−1500 cm^{-1}, **Figure 3** presents the PCA score plot using the all IR absorbance in the frequency range of 1700−1500 cm^{-1} as variables. The samples clustered according to heating rate and meat quality. The first main variation with an explained variance of 56% (PC1) and the second main variation with an explained variance of 15% (PC2) in the IR spectra were attributed to heating rate and raw meat qualities, respectively. To cover a wide range of biological variance in this study, the parallel replicates for one heating rate of each meat quality were sampled from the different locations of both right and left M. longissimus (ca. 40 cm long of each), which induced the broad spanning of parallel replicates. However, an effect of a slightly larger range of temperature which may occur on the fast heated samples cannot be ruled out.

The score plot of PCA can reveal the existence of main variation in IR spectra caused by heating rate and meat quality. To elucidate the relationship between the specific protein secondary structural changes and heating rate and meat quality, a correlation loading plot (first and second PLS component) of PLSR2 with the design (heating rate, meat quality, and interaction) as *X* and the selected IR bands in the region of 1700−1500 cm^{-1} as **Y** (negative second derivative) is presented in **Figure 4**. The slow heating rate was positively correlated with the absorption bands at 1652, 1543, 1626, 1555, and 1658 cm^{-1}, while the fast heating rate was positively related to the bands at 1695, 1642, 1534, 1610, 1620, 1510, 1525, 1566, and 1668 cm^{-1}. In comparison, meat quality had a weaker effect on protein secondary structural changes. PSE is located in the same direction as the fast heating rate, while the DFD and normal meat are located in the same direction as the slow heating rate. Moreover, the combined effect of heating rate and meat quality showed the different effect of heating rate on different meat qualities.

As indicated in the correlation loading plot, the slowly heated samples were characterized by a high content of α-helical

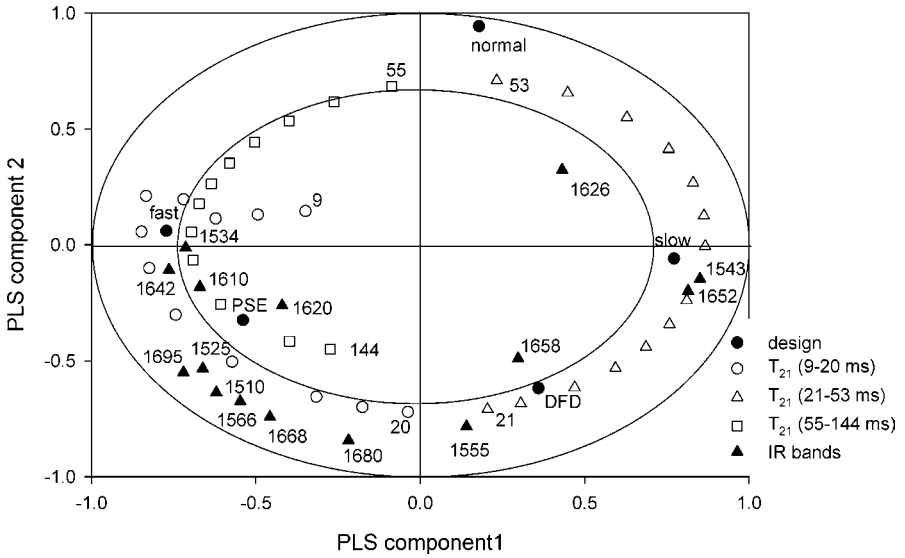

Figure 5. Correlation loading plot (first and second PLS component) of PLSR2 using design parameters and NMR relaxation times as *X* and selected frequency variables of the (negative) second derivative of FT-IR spectra in the region of 1700–1500 cm^{-1} as *Y*. The inner and outer ellipses refer to 50% and 100% explained variance in *X* and *Y*, respectively. The validated explained variances are 38%/23% for *X* and 43%/15% for *Y*, the first and the second component, respectively.

structures (1652 and 1543 cm^{-1}) and a native loop structure (1658 cm^{-1}) compared with the fast heating, indicating less loss of α-helical structures during slow heating. In comparison, fast heating causes a higher loss of α-helical structures and high gain of random structures at 1642 and 1668 cm^{-1} (*36*, *37*); aggregated *β*-sheets at 1695, 1620, 1525, and 1566 cm^{-1}; and amino acid tyrosine related to the bands at 1610 and 1510 cm^{-1}. Interestingly, two bands at 1620 and 1626 cm^{-1} arising from the aggregated intermolecular *β*-sheets showed an opposite correlation with heating rate: the band at 1626 cm^{-1} is positively related to slow heating and the band at 1620 cm^{-1} is positively related to fast heating. It has been found that the stronger the hydrogen bond involving the amide C═O, the lower the electron density in the C═O group and the lower the amide I absorption appears (*38*), which may suggest that stronger hydrogen bonds can be formed during fast heating in comparison to relatively weaker hydrogen bonds during slow heating. Moreover, as shown in **Figure 4**, different meat qualities had a different sensibility to heating rate. DFD and normal meat quality both are positively correlated to slow heating and the bands at 1652 and 1543 cm^{-1}, revealing that a slowing heating rate applied on DFD meat and normal meat quality would induce less loss of α-helical structure. The differences between DFD and normal quality are based on the opposed correlation to the bands at 1680, 1555, 1658, and 1626 cm^{-1}, while PSE meat is positively correlated to fast heating, suggesting that protein aggregation of PSE meat caused by fast heating is more extensive than that of DFD and normal meat.

In addition, the present IR results built a relationship between protein secondary structures and water content in meat upon heating rate. Fast heating induces a higher cooking loss than slow heating. On the basis of the protein secondary structural changes caused by heating rate and meat quality, it can be concluded that a high water content in meat must be related to a high content of α-helical structures, while a low water content can be ascribed to more random structures and aggregated *β*-sheet and less α-helical structures.

Relationship between Water Distribution and Protein Secondary Structure. To elucidate the relationship between water distribution, water dynamics, and protein secondary structure as affected by heating rate and raw meat quality, PLSR2 was performed using design parameters (heating rate and meat quality) and NMR T_2 relaxation times as *X* and selected frequency variables of the (negative) second derivative of FT-IR spectra in the region of 1700−1500 cm^{-1} as *Y*. **Figure 5** shows the correlation loading plot (first and second PLS component) of PLSR2, and the validated explained variances are 38%/37% for *X* and 29%/11% for *Y* by the first and the second component, respectively. In **Figure 5**, T_{21} is characterized by fast (9−19 ms), intermediate (20−53 ms), and slow relaxation parts (55−144 ms). It was observed that the slow heating rate is correlated to the α-helical structures at 1652 and 1543 cm^{-1} and T_2 relaxation times centered at 20−50 ms, implying that α-helical structures dominate the water proton T_2 relaxation times within 20−50 ms and the high moisture in meat. This is consistent with previous studies (*10*, *12*). Fast heating rate is positively correlated to aggregated *β*-sheet and random structures along with the fast and slow T_{21} relaxation parts, which reveals that the aggregated *β*-sheet and random structures predominantly contribute to the fast (9−19 ms) and slow T_{21} (55−144 ms) relaxation times and subsequently to the broadening of T_{21} distribution and the decrease in the relaxation time of the T_{21} peak position. Moreover, aggregated *β*-sheet and random structures are positively correlated to PSE meat, indicating that PSE meat has a higher susceptibility to fast heating rate, and as a result, a broader T_{21} distribution is observed in PSE meat than in DFD and normal meat. This observation could very well explain the most significant broadening of T_{21} distribution and decrease in relaxation time of the T_{21} peak position for fast heated PSE meat. As different protein structures upon heating rate and meat quality are associated with the different distribution of water proton T_2 relaxation time, this relationship verifies the hypothesis suggested in the NMR part that changes in water proton T_2 relaxation times are a sign of the protein structural changes. The demonstrated relationship between the water proton T_2 and protein structure supports the interpretation that the water protons T_2 relaxation in meat can be explained in terms of the chemical and diffusive exchange between water protons and protein protons as the correlation time of protein

protons varies depending on protein structure and conformation. Therefore, water proton T_2 relaxation time is highly related to protein structure and protons dynamics and, hence, a good indicator of water distribution, proton dynamics, and protein structures.

In conclusion, the present study demonstrated that water proton T_2 relaxation time and meat protein structure are influenced by heating rate and raw meat quality. A relationship between cooking loss, water proton T_2 relaxation time, and protein secondary structure has been established. A high content of α-helical structures upon slow heating resulted in a more narrow T_{21} distribution, a high relaxation time of the T_{21} peak position, and lower cooking loss, while on the other hand, a random structure and aggregated β-sheet contributed to a broadening of T_{21} distribution, a decrease in the relaxation time of the T_{21} peak position, and an increase of cooking loss upon fast cooking. Furthermore, of the measured parameters, fast heating of PSE meat induced the broadest water proton T_{21} distribution, the fastest relaxation time of the T_{21} peak position, and the highest cooking loss, which are well explained by the most significant protein aggregation detected by FT-IR.

LITERATURE CITED

(1) Tornberg, E. Effects of heat on meat proteins − Implications on structure and quality of meat products. *Meat Sci.* **2005**, *70*, 493−508.

(2) Aaslyng, M. D.; Bejerholm, C.; Ertbjerg, P.; Bertram, H. C.; Andersen, H. J. Cooking loss and juiciness of pork in relation to raw meat quality and cooking procedure. *Food Qual. Pref.* **2003**, *14*, 277−288.

(3) Appel, D.; Löfqvist, B. Meat cooking techniques—Part 1: A preliminary study of the effect of the rate of heating in water. *Meat Sci.* **1978**, *2*, 251−262.

(4) Abugroun, H. A.; Forrest, J. C.; Aberle, E. D.; Judge, M. D. Shortening and tenderness of pre-rigor heated beef: Part 2 — Effect of heating rate on muscles of electrically stimulated carcasses. *Meat Sci.* **1985**, *14*, 15−28.

(5) Mortensen, M.; Andersen, H. J.; Engelsen, S. B.; Bertram, H. C. Effect of freezing temperature, thawing and cooking rate on water distribution in two pork qualities. *Meat Sci.* **2006**, *72*, 34−42.

(6) Brewer, M. S.; Novakofski, J. Cooking rate, pH and final endpoint temperature effects on color and cook loss of a lean ground beef model system. *Meat Sci.* **1999**, *52*, 443−451.

(7) Abugroun, H. A.; Forrest, J. C.; Aberle, E. D.; Judge, M. D. Shortening and tenderness of pre-rigor heated beef: Part 1 — Effect of heating rate on muscles of youthful and mature carcasses. *Meat Sci.* **1985**, *14*, 1−13.

(8) King, D. A.; Dikeman, M. E.; Wheeler, T. L.; Kastner, C. L.; Koohmaraie, M. Chilling and cooking rate effects on some myofibrillar determinants of tenderness of beef. *J. Anim. Sci.* **2003**, *81*, 1473−1481.

(9) Kirschner, C.; Ofstad, R.; Skarpeid, H.-J.; Høst, V.; Kohler, A. Monitoring of denaturation processes in aged beef loin by Fourier transform infrared microspectroscopy. *J. Agric. Food Chem.* **2004**, *52*, 3920−3929.

(10) Bertram, H. C.; Kohler, A.; Böcker, U.; Ofstad, R.; Andersen, H. J. Heat-induced changes in myofibrillar protein structures and myowater of two pork qualities. A combined FT-IR spectroscopy and low-field NMR relaxometry study. *J. Agric. Food Chem.* **2006**, *54*, 1740−1747.

(11) Böcker, U.; Ofstad, R.; Bertram, H. C.; Egelandsdal, B.; Kohler, A. Salt-induced changes in myofibrillar tissue of different pork qualities investigated by FT-IR microspectroscopy and light microscopy. *J. Agric. Food Chem.* **2006**, *54*, 6733−6740.

(12) Wu, Z.; Bertram, H. C.; Kohler, A.; Böcker, U.; Ofstad, R.; Andersen, H. J. Influence of aging and salting on protein secondary structures and water distribution in non-cooked and cooked pork. A combined FT-IR micro-spectroscopy and ^{1}H NMR relaxometry study. *J. Agric. Food Chem.* **2006**, *54*, 8589−8597.

(13) Bertram, H. C.; Andersen, H. J. Applications of NMR in Meat Science. *Annu. Rep. NMR Spectrosc.* **2004**, *53*, 157−202.

(14) Henckel, P.; Karlsson, A.; Oksbjerg, N.; Petersen, J. S. Control of post mortem decrease in pig muscles: experimental design and tesing of animal models. *Meat Sci.* **2000**, *55*, 131−138.

(15) Honikel, K. O. Reference methods for the assessment of physical characteristics of meat. *Meat Sci.* **1998**, *49*, 447−457.

(16) Martens, H.; Stark, E. Extended multiplicative signal correction and spectral interference subtraction - new preprocessing methods for near-infrared spectroscopy. *J. Pharm. Biomed. Anal.* **1991**, *9*, 625−635.

(17) Kohler, A.; Kirschner, C.; Oust, A.; Martens, H. Extended multiplicative signal correction as a tool for separation and characterization of physical and chemical information in Fourier Transform Infrared microscopy images of cryo-sections of beef loin. *Appl. Spectrosc.* **2005**, *59*, 707−716.

(18) Martens, H.; Martens, M. *Multivariate Analysis of Quality: An Introduction*; John Wiley & Sons, Ltd: Chichester, U.K., 2001.

(19) Oust, A.; Moen, B.; Martens, H.; Rudi, K.; Næs, T.; Kirschner, C.; Kohler, A. Analysis of co-variation patterns in gene expression data and FT-IR spectra, *J. Microbiol. Methods* **2005**, *65*, 573−584.

(20) Tornberg, E.; Andersson, A.; Göransson, Å.; von Seth, G. Water and Fat Distribution in Pork in Relation to Sensory Properties. In *Pork Quality: Genetic and Metabolic Factors*; Puolanne, E., Demeyer, D. I., Ruusunen, M., Ellis, S., Eds.; CAB International, 1993.

(21) Offer, G. Modelling of the formation of pale, soft and exudative meat: effects of chilling regime and rate and extent of glycolysis. *Meat Sci.* **1991**, *30*, 157−184.

(22) Warner, R. D.; Kaufman, R. G.; Greaser, M. L. Muscle protein changes post mortem in relation to pork quality traits. *Meat Sci.* **1997**, *45*, 339−352.

(23) Fischer, C.; Hamm, R.; Honikel, K. O. Changes in solubility and enzymic activity of muscle glycogen phosphorylase in PSE-muscles. *Meat Sci.* **1979**, *3*, 11−19.

(24) Warriss, P. D.; Brown, S. N. The relationships between initial pH, reflectance and exudation in pig muscle. *Meat Sci.* **1987**, *20*, 65−74.

(25) Barbut, S.; Zhang, L.; Marcone, M. Effects of pale, normal, and dark chicken breast meat on microstructure, extractable proteins, and cooking of marinated fillets. *Poult. Sci.* **2005**, *84*, 797−802.

(26) Bertram, H. C.; Purslow, P. P.; Andersen, H. J. Relationship between meat structure, water mobility, and distribution: A low-field nuclear magnetic resonance study. *J. Agric. Food Chem.* **2002**, *50*, 824−829.

(27) Tornberg, E.; Andersson, A.; Goransson, A.; von Seth, G. *Pork Quality: Genetic and Metobolic Factors*; CAB International: U.K.; p 239.

(28) Bertram, H. C.; Aaslyng, M. D.; Andersen, H. J. Elucidation of the relationship between cooking temperature, water distribution and sensory attributes of pork - a combined NMR and sensory study. *Meat Sci.* **2005**, *70*, 75−81.

(29) Hills, B. P.; Takacs, S. F.; Belton, P. S. The effect of proteins on the proton NMR transverse relaxation time of water II Protein aggregation. *Mol. Phys.* **1989a**, *67*, 919−937.

(30) Hills, B. P.; Wright, K. M.; Belton, P. S. NMR studies of water proton relaxation in sephadex bead suspensions. *Mol. Phys.* **1989b**, *67*, 193−208.

(31) Belton, P. S.; Hills, B. P.; Raimbaud, E. The effect of morphology and exchange on proton NMR relaxation times in agarose gels. *Mol. Phys*. **1988**, *63*, 825−842.
(32) Belton, P. S. NMR and the mobility of water in polysaccharide gels. *Int. J. Biol. Marcromol.* **1997**, *21*, 81−88.
(33) Dean, A. L.; Mariette, F.; Marin, M. 1H nuclear magnetic resonance relaxometry study of water state in milk protein mixtures. *J. Agric. Food Chem*. **2004**, *52*, 5449−5455.
(34) Nevskaya, N. A.; Chirgadze, Y. N. Infrared spectra and resonance interactions of amide-I and II vibrations of α -helix. *Biopolymers* **1976**, *15*, 637−648.
(35) Çakmak, G.; Togan, I.; Uğuz, C.; Severcan, F. FT-IR Spectroscopic Analysis of Rainbow Trout Liver Exposed to Nonylphenol. *Appl. Spectrosc.* **2003**, *57*, 835−841.
(36) Goormaghtight, E.; Cabiaux, V.; Ruysschaert, J. M. In *Subcellular Biochemistry*; Hilderson, H. J., Ralston, G. B., Eds.; Plenum Press: New York, 1994; Vol. 23.
(37) Sokrates, G. *Infrared and Raman Characteristic Group Frequencies. Tables and Charts*, 3rd ed.; John Wiley & Sons Ltd.: Chichester, U.K., 2001.
(38) Jackson, M.; Mantsch, H. H. The use and misuse of FTIR spectroscopy in the determination of protein-structure. *Crit. Rev. Biochem. Mol. Biol.* **1995**, *30*, 95−120.

Received for review January 3, 2007. Revised manuscript received March 15, 2007. Accepted March 22, 2007. Financial support by the Danish Meat and Bacon Council for funding the project "Process-induced structural changes in muscle proteins of importance for functional properties of meats" by Grant 153381/140 from the Norwegian Research Council, and the Fund for Research Levy on Agricultural Products is gratefully acknowledged.

JF070019M